An Accurate and Flexible Calorimeter Topology for Power Electronic System Loss Measurement

Nick Simpson[1] and Andrew N. Hopkins[1]
[1]Department of Electrical and Electronic Engineering, University of Bristol, Bristol, UK, nick.simpson@bristol.ac.uk

***Abstract*—The drive to improve power electronic system efficiencies makes the accurate and repeatable determination of power losses ever more important. As operating frequencies, harmonic content and efficiency increase, electrical methods of measuring loss become more uncertain since they are affected by phase-errors and electromagnetic interference among other factors. Alternative calorimetric methods allow system losses, which manifest as heat, to be measured directly with a high degree of accuracy. However, calorimeter facilities tend to be costly bespoke measurement systems which is a barrier to their widespread use. In this paper, an extension to the closed double-jacket type calorimeter topology is presented which offers comparatively low-cost, simplified construction and improved flexibility with the aim of promoting a more widespread use of calorimetry within the power electronics community.**

Index Terms*—calorimeter, closed surface-heated topology, loss measurement, power electronic system

I. Introduction

The accurate and repeatable determination of power losses is of great importance to the design, optimisation and performance evaluation of power electronic systems and components, [1], [2]. However, the measurement of losses becomes more challenging with increasing operating frequencies, harmonic content and efficiency, [3], [4].

Electrical measurement methods use the product of voltage and current at the input and output of a Device Under Test (DUT) to indirectly yield input and output power P_{in} and P_{out} respectively. The difference in power (1) gives the power loss P_{loss} and the ratio (2) gives the efficiency, η. In the measurement of high-efficiency systems, where the input and output power are similar in magnitude, phase-errors and Electromagnetic Interference (EMI), among other factors can lead to unacceptable inaccuracies in loss and efficiency measurements, [2]–[4].

$$P_{loss} = P_{in} - P_{out} \tag{1}$$

$$\eta = \frac{P_{out}}{P_{in}} \tag{2}$$

Calorimetric measurement methods offer an alternative in which the losses from the DUT, manifesting as heat, are measured directly. Numerous specialist calorimeter topologies exist suitable for the measurement of power transformer losses, [5], magnetic core material losses, [6], Integrated Power Electronic Module (IPEM) losses, [7], capacitor losses [8] and power analyser calibration, [9]. General purpose calorimeter topologies applicable to power electronic systems and electrical machines typically take the form of open, Fig. 1, or closed, Fig. 2, type calorimeters, [4], [10].

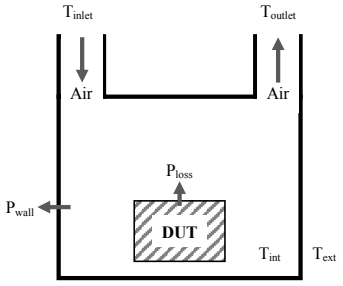

Fig. 1. Open calorimeter topology.

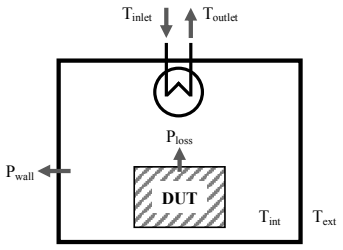

Fig. 2. Closed calorimeter topology.

In principle, the DUT is placed within an insulated chamber and the DUT losses are absorbed by a cooling medium while the flow rate $\dot{V}$ and temperature rise ΔT are measured in the steady state. If ideal insulation is assumed and no heat leakage occurs, the losses are given by (3), where c_p and ρ are the specific heat capacity and mass density of the cooling medium respectively.

$$P_{loss} = c_p \rho \dot{V} \Delta T = c_p \rho \dot{V} \left(T_{outlet} - T_{inlet}\right) \tag{3}$$

The open type calorimeter uses fan blown air as the cooling medium whilst the closed type uses pumped liquid such as water and a heat exchanger arrangement which adds to system complexity. However, the specific heat capacity and density of a fluid system are less sensitive to changes in temperature than air and the higher heat capacity allows physically smaller components and lower flow velocities to be used which eases flow rate measurement and improves accuracy, [4]. In both calorimeter types, the accuracy of the power measurement is negatively affected by heat leakage through non-ideal thermal

insulation which is a function of the difference in internal T_{int} and external temperature T_{ext} and the effective thermal resistance R_{th} of the chamber, (4). The effect of heat leakage on the power measurement could be mitigated by performing a balance test using a dc load at the cost of doubling the measurement time requirement, [10].

$$P_{loss} = \underbrace{c_p \rho \dot{V} \left(T_{outlet} - T_{inlet}\right)}_{\text{Power absorbed by cooling medium}} + \underbrace{\frac{T_{int} - T_{ext}}{R_{th}}}_{\text{Heat leakage}} \quad (4)$$

Alternatively, heat leakage can be minimised by increasing the insulation thickness (R_{th}), however, this approach undesirably increases the thermal time constant of the system and consequently the settling time required for a steady state power measurement, [1]. This problem is partially addressed by the closed double-jacket calorimeter topology, Fig. 3 in which an outer chamber is used to form a heated air-gap, [11], [12]. The air-gap temperature T_{ext} is controlled to match the internal chamber temperature T_{int} to reduce heat leakage, theoretically to zero, (4).

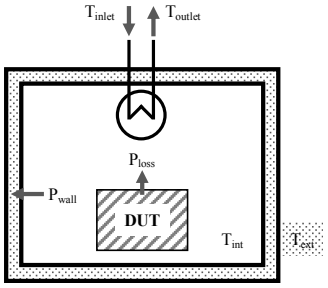

Fig. 3. Closed Double-Jacket calorimeter topology.

The closed double-jacket calorimeter topology is shown to offer the highest measurement accuracy, [1], [4], [11], [12]. However, the implementation of such a calorimeter is complex and costly due to the requirement of two nested chambers, a temperature controlled air-gap, the use of a fluid cooling system and difficulty in passing fluid and electrical connections through the chamber walls, [1], [2], [12]–[14]. In addition, it is often prudent to size the calorimeter chambers to meet future needs which leads to a mismatch in chamber and DUT volume resulting in sub-optimal measurement performance.

In this paper, an extension to the closed double-jacket calorimeter topology is presented which addresses several of the aforementioned disadvantages:

- The measurement chamber is based on a single low-cost pre-fabricated polystyrene box selected to match a particular DUT volume.
- The external surface of the measurement chamber is heated by a low-cost surface heater to minimise heat leakage and reduce steady-state power measurement time.
- Reusable bulkhead connectors are used to pass fluid and electrical connections through the chamber walls whilst minimising heat leakage.
- The fluid cooling system is constructed using commercially available computer cooling components.
- All measurement apparatus, e.g. data acquisition boards, power supplies and temperature sensors are commercially available.
- The measurement chamber is decoupled from the measurement apparatus enabling one set of apparatus to be used across multiple measurement chambers of varying sizes suited to a range of DUT envelopes.

A prototype closed surface-heated calorimeter is constructed to meet the specification given in Table I. The measurement performance of the topology is established by comparing the calorimeter power measurements of a dc load with those obtained by a precision power analyser with a known accuracy.

TABLE I
CALORIMETER SPECIFICATION.

Parameter	Value	Unit
DUT width (minimum)	75	mm
DUT height (minimum)	100	mm
DUT length (minimum)	175	mm
Minimum power measurement	20	W
Maximum power measurement	≥ 100	W
Measurement accuracy	≤ 2	%

II. CLOSED SURFACE-HEATED CALORIMETER TOPOLOGY

A schematic of the proposed closed surface-heated calorimeter topology and the associated measurement apparatus and fluid cooling system is illustrated in Fig. 4. The calorimeter is composed of three connected subsystems, the measurement chamber, the fluid cooling system and the data acquisition and control system. Each subsystem is treated in turn.

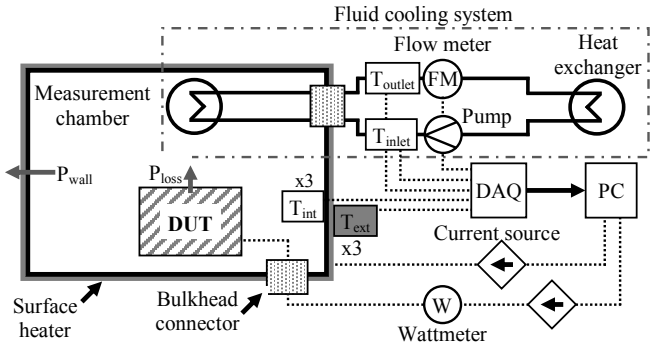

Fig. 4. Schematic of the proposed Closed Surface-Heated calorimeter topology and associated measurement apparatus and fluid cooling system.

A. Measurement Chamber

Measurement chambers are often built using a structural frame and double layers of sheet insulation material in order to ensure an air-tight construction that meets a certain wall thickness and chamber volume, [1]. Here, an air-tight commercially available JBP Expanded Polypropylene (EPP)

container is employed to reduce overall cost and construction complexity, Fig. 5. The internal dimensions of the container are $525 \times 305 \times 195$ mm matched to the DUT specification, Table I, allowing for the additional space requirement of the heat exchanger and bulkhead connectors. The container has a 30 mm wall thickness with a thermal conductivity of 0.04 W/m.K resulting in an effective thermal resistance, R_{th}, of 1.17 ^{o}C/W.

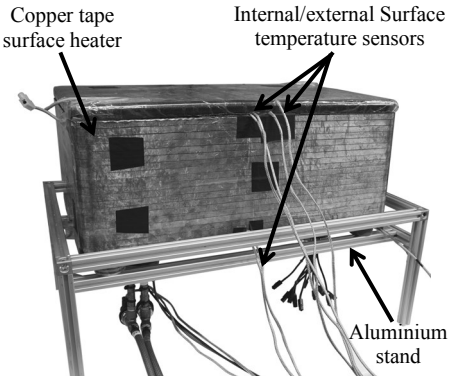

Fig. 5. External view of measurement chamber.

The external surface of the measurement chamber is heated using 10×0.035 mm copper tape with a non-conductive adhesive backing which forms a low-cost surface heater. The tape is wound around the periphery of the measurement chamber to create a continuous strip heater, Fig. 5 and then applied in a regular alternating pattern to the top and bottom surfaces leaving uncovered areas sufficient for the bulkhead connectors. The heater power of the top, bottom and sides of the measurement chamber can be controlled independently or they can be connected in series or parallel and driven from a single power supply. The copper strips are physically separated by a gap of approximately 0.25 mm and a clear polyester film tape with a temperature rating of 130 ^{o}C is applied to electrically insulate the copper tape and reliably maintain spacing between the strips. Electrical connectors are soldered directly to the copper tape. When connected in series, the surface heater has a resistance of 3.9 Ω or $4.5\ \Omega/m^2$. The inner surface of the chamber is covered with overlapping layers of 50×0.05 mm adhesive aluminium tape to aid a homogeneous temperature distribution, Fig. 7. The inner and outer chamber surface temperatures (side, top and bottom) are measured using 3 mm diameter $\times$ 50 mm 4-wire class A PT100 Resistance Temperature Detector (RTD) probes inserted directly into the polypropylene approximately 1 mm beneath the surface.

In order to make the measurement chamber flexible and reusable, the fluid, power and signal connections must breach the chamber walls without the need for permanent sealing or adhesion. This is achieved using threaded 63.5 mm Enduramaxx plastic tank outlets to create custom bulkhead connectors. The tank outlets are sealed using laser cut perspex end-plates adhered to each end. The end-plates feature cut-outs

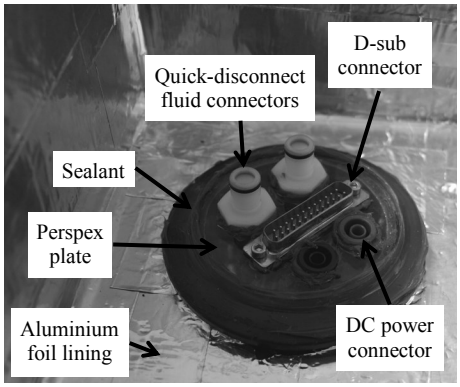

Fig. 6. Internal view of bulkhead connector (fluid, power).

for the necessary panel mount connectors, Figs. 6 and 7.

One bulkhead connector is dedicated to the fluid cooling system and provides inlet and outlet quick-disconnect fluid connections, 2×24 A, 4 mm sockets for DC load (balance) testing, and a 25-pin D-sub connector for fan power and future signal and power requirements, section II-B and Figs. 6 and 7.

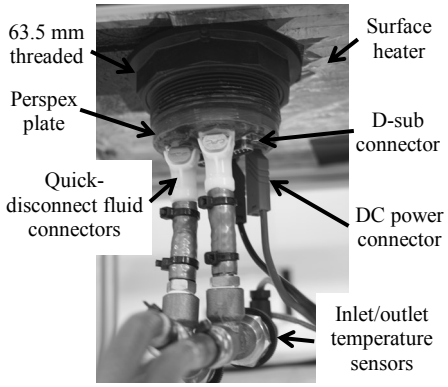

Fig. 7. External view of bulkhead connector (fluid, power).

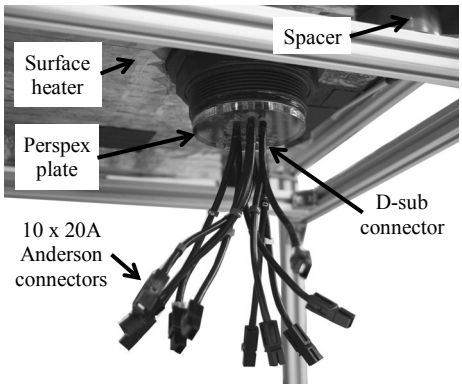

Fig. 8. External view (DUT connections).

A second bulkhead connector is dedicated to the DUT connections and features a 15-pin D-sub connector for signal and low power connections along with 10×30 A multicomp BMC power connections. The bulkhead connectors are inserted into

75 mm hole-saw cut openings in the measurement chamber base and secured using the corresponding threaded nut and rubber gaskets to provide air-tight seals, Fig. 8.

B. Fluid Cooling System

A schematic of the fluid cooling system is illustrated in Fig. 9 where standard computer cooling components are used to transfer the DUT losses from the measurement chamber to the ambient atmosphere in a controlled manner. The internal heat exchanger is a 120×240 mm XSPC EX240, mounted with $2\times$ Corsair SP120 fans used to aid the heat exchange and homogenisation of the air temperature within the measurement chamber, Fig. 10. The external heat exchanger arrangement is a series combination of $2\times$ XSPC EX240 heat exchangers each mounted with $2\times$ Corsair SP120 fans to provide forced convection. The fans are electrically connected in parallel to a fixed 12 V power supply. The fan power is measured in situ using a Norma 4000 high precision power analyser and subtracted from the calorimeter power measurements in the control software, section II-C.

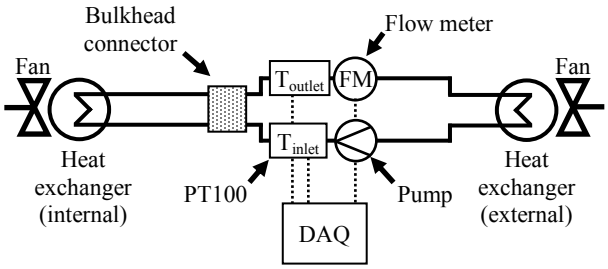

Fig. 9. Schematic of the calorimeter fluid cooling system.

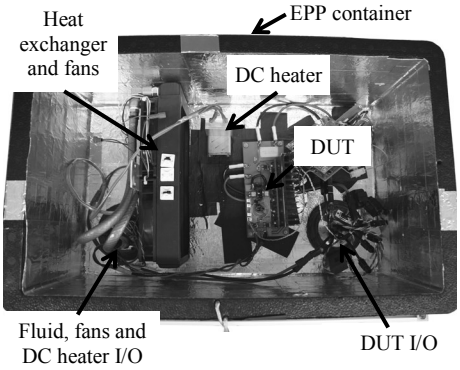

Fig. 10. Internal view of measurement chamber.

The fluid (distilled water) is pumped around the cooling loop using a Watson Marlow 505U rotary peristaltic pump which provides high static pressure, self priming ability and stable low-medium flow rates. In addition, the fluid carrying and moving pump components are isolated which simplifies priming, cleaning and maintenance of the system. The theoretical flow rate of the peristaltic pump, $\dot{V}_{pump}$, is given in terms of the occluded volume and length of tubing, V_{tubing}, L_{tubing}, the number of rollers, $N_{rollers}$ and the rotational speed, v, (5), [15].

$$\dot{V}_{pump} = V_{tubing} L_{tubing} N_{rollers} v \tag{5}$$

The fluid flow rate is measured using a low-cost DigiFlow 6710M-34TM flow rate sensor with a rated measurement range of $0.05 - 1.0$ l/min and a $\pm 10\%$ accuracy which would have a detrimental impact on power measurement accuracy, (4). Therefore, the fluid cooling system includes a valve arrangement to enable the flow rate sensor to be calibrated in situ by weighing the fluid discharged over a fixed time period at various pump speeds (flow rates) using a Kern PCB 6000-1 precision balance. The relationship between the number of electrical output pulses and fluid volume flow rate is sown in Fig. 11. The manufacturer data is shown with $\pm 10\%$ error bars along with measured calibration data. The measured data is lower than that suggested by the manufacturer, however, a linear relationship is maintained above 100 ml/min with a coefficient of determination, R^2, of 0.99. At flow rates below 100 ml/min the flow rate sensor rotor stalls and gives unreliable, intermittent readings, [16]. Hence, the minimum flow rate used by the prototype calorimeter is 100 ml/min. The theoretical flow rate expression, (5), and the pump speed are used to validate the measured flow rate during calorimeter operation.

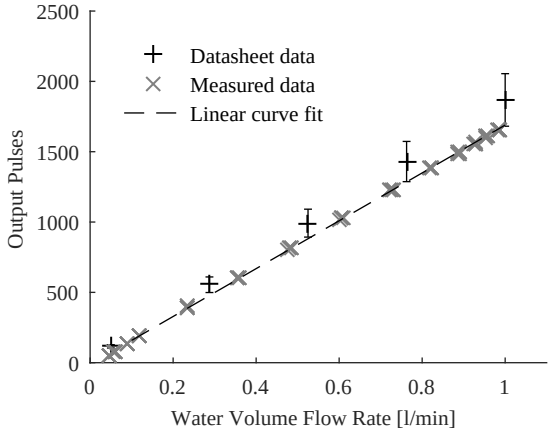

Fig. 11. Calibration of the flow rate sensor.

The inlet and outlet fluid temperatures, T_{inlet} and T_{outlet}, are measured using Jumo 4-wire class A PT100 RTDs mounted with the probes submerged in the cooling fluid, Fig. 7. Each RTD in the system has an accuracy of $\pm\,(0.15 + 0.002T)$ ^{o}C with a maximum operating temperature of 90 ^{o}C dictated by the rated operating temperature of the insulation materials with an appropriate margin.

C. Data Acquisition and Control System

The temperature sensor signals are acquired using a Measurement Computing USB-TEMP and the flow rate sensor pulses are acquired using a Measurement Computing USB-1208FS pulse counter. The pump speed is controlled using an analog voltage supplied by the USB-1208FS. The surface heater is powered by a TTI CPX400DP controllable power

supply. All sensor leads are screened and the DAQ hardware is housed inside a shielded enclosure in order to minimise the impact of EMI on the system. A PC based software controller provides a Graphical User Interface (GUI) and reads the temperature and flow rate data from the DAQ hardware. During operation, the pump speed is controlled to maintain a user defined operating temperature of the measurement chamber (above ambient) using a software Proportional Integral (PI) controller which allows the DUT to be tested under realistic operating temperatures. The surface heater is PI controlled to ensure that the difference in internal and external surface temperature is minimised to reduce heat leakage. The acquired data is used to perform power calculations, (4), and display the results in real time. Sliding window filtering is used on the flow rate sensor data to mitigate pulsations caused by the peristaltic pump rollers. Thermal steady state is detected automatically from the relative change in temperature data.

III. Calibration and Experimental Testing

The prototype calorimeter and associated measurement apparatus are shown in Fig. 12. Careful design choices have been made at each stage of the prototype development in order to minimise sources of error and heat leakage whilst maintaining low-cost and complexity.

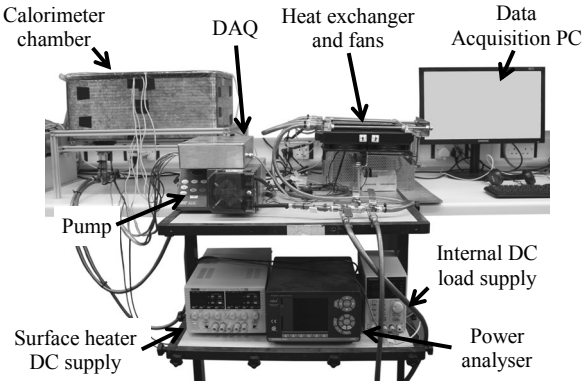

Fig. 12. Calorimeter and apparatus setup.

However, unaccounted heat paths exist through the electrical connections and through the bulkhead connectors, the series connected surface heater can produce non-uniform heating and the temperature sensors and associated DAQ hardware exhibit offsets and uncertainty. The desired accuracy of the calorimeter is $\leq 2\%$ with a minimum measurement of 20 W, hence the heat leakage P_{wall} must be less than 0.4 W, (6). As a result the surface and internal measurement chamber temperature must be controlled within less than 0.47 ^{o}C, section II-A, [4]. It is therefore essential to perform a calibration procedure using a power measurement method with a known accuracy in order to account for the build factors and signal offsets of the prototype calorimeter implementation.

$$|T_{int} - T_{ext}| < P_{wall} R_{th} \tag{6}$$

A single-point calibration was performed by comparing measurements of the power applied to a DC load obtained using the calorimeter to measurements obtained using a Norma 4000 high precision power analyser with a 4-wire configuration. A nominal DC power of 50 W was used, measured to be 49.76 W $\pm 0.4\%$ using the Norma 4000. The internal measurement chamber was controlled and maintained at 30 ^{o}C. In the steady-state, the difference in power measured using the calorimeter and the power analyser was minimised by setting appropriate temperature sensor offsets and stray heat leakage parameters within the PC software. In the current implementation the parameters are selected and applied manually. The calorimeter and electrical power measurement at the calibration point is shown in Fig. 13. The calorimeter power measurement error was reduced from 1.5 W to 0.21 W by the calibration process.

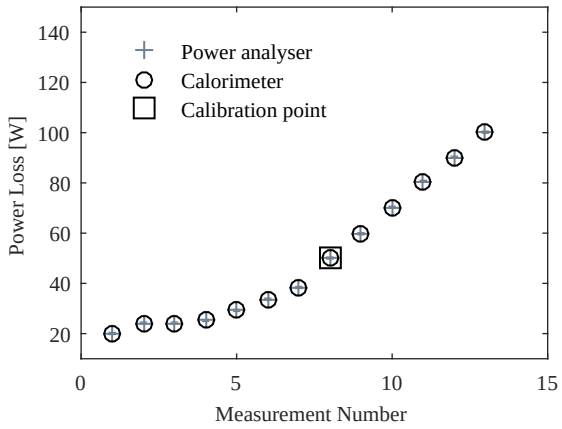

Fig. 13. Absolute power measurements including one calibration point.

Using the single-point calibration data, the calorimeter was tested at 12 unique DC load points in the range 20-100 W, Table I, and plotted in Fig. 13. In each instance the measurement reached steady-state in under two hours. The calorimeter power measurements exhibit a percentage error of $\epsilon_{percent} < 1\%$ in all cases up to 100 W, Fig. 14. This corresponds to an absolute error of $\epsilon_{absolute} < 0.4$ W when compared to power analyser measurements and is lower than the 2% error demanded by the specification, Table I.

The trend of the measurement error $\epsilon_{percent}$ increases as the DUT power decreases, Fig. 14. At the minimum 20 W measurement point the flow rate is 127 ml/min, approaching the minimum allowable flow rate of 100 ml/min established in section II-B. In addition, the peristaltic pump operates below 10 rpm with a speed controller resolution of 1 rpm which has a significant impact on the measurement chamber temperature control. The minimum measurement chamber temperature is limited by the ambient temperature since the fluid cooling system and surface cooling is passive. Hence, the measurement chamber temperature must sufficiently exceed the ambient temperature to provide adequate cooling performance and an inlet and outlet water temperature differential greater than the measurement error associated with the RTDs and DAQ

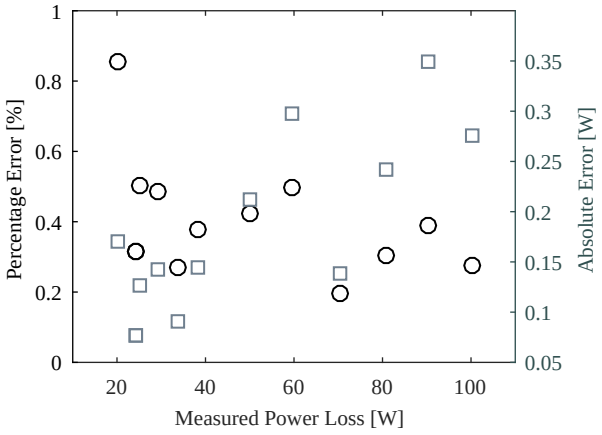

Fig. 14. Comparison of power analyser and calorimeter power measurements.

hardware. The calorimeter was calibrated and subsequently tested at a measurement chamber temperature of 30 ^{o}C. The surface temperature measurements from the top, bottom and sides are averaged and the surface heaters connected in series in order to simplify control and power requirements. However, the orientation and surface area of each face varies. Hence the performance of the surface heater may degrade when tested with alternative measurement chamber temperatures. Individual surface heater control could result in a greater level of loss minimisation suited to a wide range of measurement chamber operating temperatures.

Extending the power measurement below 20 W without significantly compromising accuracy would require a physically smaller measurement chamber, a more accurate flow rate sensor and a pump with a higher resolution speed controller. The upper power measurement limit is dictated by the maximum flow rate. With the current configuration an upper limit of 250 W is anticipated.

The prototype calorimeter has been tested at a number of DUT power levels at 30 ^oC over a 20-100 W range and exhibits a measurement accuracy below 1 $\%$ when compared to power analyser measurements.

IV. Conclusion

This paper presents a closed surface-heated calorimeter topology which is an extension of the closed double-jacket topology, [11], [12]. The topology offers relatively low-cost, a simple measurement chamber construction and significantly improved flexibility as the measurement chambers are reusable, decoupled from the measurement apparatus and enable a DUT to be tested at a specified measurement chamber temperature, section II. A prototype calorimeter was constructed to meet the specification set out in Table I. Experimental tests show that the prototype exceeds the specification exhibiting a measurement error below 1 $\%$ over the range 20-100 W with a measurement chamber temperature of 30 ^oC. The calorimeter was calibrated using a single DC load test. Future work will focus on a statistical assessment of the calorimeter measurement performance, improving the low power measurement capability and an investigation of individual surface heater control to maintain the measurement accuracy over a range of measurement chamber temperatures. This research aims to promote a more widespread use of calorimetry within the power electronics community.

References

[1] D. Christen, U. Badstuebner, J. Biela, and J. W. Kolar, "Calorimetric power loss measurement for highly efficient converters," in *The 2010 International Power Electronics Conference - ECCE ASIA -*, June 2010, pp. 1438–1445.

[2] A. Kosonen, L. Aarniovuori, J. Pyrhönen, M. Niemelä, and J. Backman, "Calorimetric concept for measurement of power losses up to 2 kw in electric drives," *IET Electric Power Applications*, vol. 7, no. 6, pp. 453–461, 2013.

[3] L. Aarniovuori, A. Kosonen, P. Sillanpää, and M. Niemelä, "High-power solar inverter efficiency measurements by calorimetric and electric methods," *IEEE Transactions on Power Electronics*, vol. 28, no. 6, pp. 2798–2805, 2013.

[4] C. Xiao, G. Chen, and W. G. H. Odendaal, "Overview of power loss measurement techniques in power electronics systems," *IEEE Transactions on Industry Applications*, vol. 43, no. 3, pp. 657–664, May 2007.

[5] J. K. Bowman, R. F. Cascio, M. P. Sayani, and T. G. Wilson, "A calorimetric method for measurement of total loss in a power transformer," in *Power Electronics Specialists Conference, 1991. PESC '91 Record., 22nd Annual IEEE*, Jun 1991, pp. 633–640.

[6] R. Linkous, A. W. Kelley, and K. C. Armstrong, "An improved calorimeter for measuring the core loss of magnetic materials," in *APEC 2000. Fifteenth Annual IEEE Applied Power Electronics Conference and Exposition (Cat. No.00CH37058)*, vol. 2, 2000, pp. 633–639 vol.2.

[7] G. Chen, C. Xiao, and W. Odendaal, "An apparatus for loss measurement of integrated power electronics modules: Design and analysis," in *Industry Applications Conference, 2002. 37th IAS Annual Meeting. Conference Record of the*, vol. 1. IEEE, 2002, pp. 222–226.

[8] B. Seguin, J. Gosse, A. Sylvestre, P. Fouassier, and J. Ferrieux, "Calorimetric apparatus for measurement of power losses in capacitors," in *Instrumentation and Measurement Technology Conference, 1998. IMTC/98. Conference Proceedings. IEEE*, vol. 1. IEEE, 1998, pp. 602–607.

[9] D. F. Frost and D. A. Howey, "High-speed peltier calorimeter for the calibration of high-bandwidth power measurement equipment," *IEEE Transactions on Instrumentation and Measurement*, vol. 65, no. 1, pp. 155–163, Jan 2016.

[10] W. Cao, G. M. Asher, X. Huang, H. Zhang, I. French, J. Zhang, and M. Short, "Calorimeters and techniques used for power loss measurements in electrical machines," *IEEE Instrumentation Measurement Magazine*, vol. 13, no. 6, pp. 26–33, December 2010.

[11] P. D. Malliband, D. R. H. Carter, B. M. Gordon, and R. A. McMahon, "Design of a double-jacketed, closed type calorimeter for direct measurement of motor losses," in *1998 Seventh International Conference on Power Electronics and Variable Speed Drives (IEE Conf. Publ. No. 456)*, Sep 1998, pp. 212–217.

[12] P. D. Malliband, N. P. van der Duijn Schouten, and R. A. McMahon, "Precision calorimetry for the accurate measurement of inverter losses," in *The Fifth International Conference on Power Electronics and Drive Systems, 2003. PEDS 2003.*, vol. 1, Nov 2003, pp. 321–326 Vol.1.

[13] F. Blaabjerg, J. K. Pedersen, and E. Ritchie, "Calorimetric measuring systems for characterizing high frequency power losses in power electronic components and systems," in *Conference Record of the 2002 IEEE Industry Applications Conference. 37th IAS Annual Meeting (Cat. No.02CH37344)*, vol. 2, Oct 2002, pp. 1368–1376 vol.2.

[14] R. Kamei, T.-W. Kim, and A. Kawamura, "Accurate calorimetric power loss measurement for efficient power converters," in *IECON 2011 - 37th Annual Conference of the IEEE Industrial Electronics Society*, Nov 2011, pp. 1173–1178.

[15] A. Kommu, R. R. Kanchi, and N. K. Uttarkar, "Design and development of microcontroller based peristaltic pump for automatic potentiometric titration," in *2014 International Conference on Communication and Signal Processing*, April 2014, pp. 157–161.

[16] B. Nakra and K. Chaudhry, *Instrumentation, measurement and analysis*. Tata McGraw-Hill Education, 2003.